5. OCEAN COLOUR REMOTE SENSING: MEASUREMENTS OF WATER-LEAVING REFLECTANCE AND WATER CONSTITUENTS

Martin Hieronymi[1], Peter Gege[2], Marcel König[3], Andreas Macke[4], Natascha Oppelt[3], Thomas Ruhtz[5]

[1]HZG
[2]DLR
[3]CAU
[4]TROPOS
[5]FUB

Grant-No. AWI_PS106/1_2-00

Objectives

a) Determination of reflectance properties of the atmosphere-ocean interface

Satellite remote sensing of ocean colour provides large-scale and global monitoring of the marine biomass and other water constituents. It is particularly suited for observations of remote and difficult accessible areas such as the North Atlantic and the Arctic Ocean. But, the higher the latitudes the more difficult is the atmospheric correction of the ocean colour signal, especially with the low sun elevation angle, the consequently longer path of radiance through the atmosphere, and increased reflectance at the sea surface. Reflectance (and transmittance) properties of the sea surface depend on the incidence angle of radiance and wind-dependent roughness of the surface, where the latter is even more important in the high-wind regions of the high latitudes. Objectives of the campaign were to measure the radiance distribution of sun and sky light in combination with the underwater light field. One focus was to study the degree of polarization of the downwelling light field. The final aim is to compare different instrumentations and their measurements with theoretically determined polarized reflectance properties of the sea surface (Hieronymi, 2016), as well as vector radiative transfer models as MOMO (Hollstein and Fischer, 2012) and the water colour simulator WASI (Gege, 2004). One additional aim of this study is to provide a better sea surface reflectance factor, which is used to determine the water-leaving radiance and remote sensing reflectance, which in turn is basis for satellite remote sensing of ocean colour.

b) Determination of optically-active water constituents

The water colour is determined by spectral absorption and scattering properties of water constituents: pure sea water, phytoplankton, coloured dissolved organic matter (CDOM), and non-algae particles. Water samples from the upper mixed layer (<5 m) should be collected and directly analysed in the laboratory. The aim is to determine the main quantities of ocean colour: inherent optical properties of the water samples as well as concentration of chlorophyll (biomass).

c) Validation of Ocean Colour algorithms and match-ups with Sentinel-3/OLCI

The remote sensing group at HZG is part of the Sentinel-3 validation team, and therefore aims to achieve match-ups with Sentinel-3 and the sensor OLCI (Ocean and Land Colour Imager)

with contemporaneous *in-situ* sampling. The first of a new satellite series, Sentinel-3A, was launched early 2016. Real match-ups are difficult to accomplish; the scenery must be cloud free and the sampling must occur ±3 h of the satellite imagery. The expedition is interesting for validation purposes because of infrequent sampling in this sea area. Furthermore, chances of match-ups increase in higher latitudes since the polar-orbiting satellite passes the ship position up to six times per day. OLCI provides data with 300 m spatial resolution. Thus, there was a chance to observe areas between ice fields and study adjacency effects as well.

The radiometric measurements serve as validation of the atmospheric correction of OLCI scenery, i.e., the retrieved remote sensing reflectance (at the sea surface). The associated water sampling serves the validation of ocean colour retrievals, in particular the new neural network based algorithm ONNS by Hieronymi et al. (2017). The final aim is to extend the exploitability of satellite imagery in high latitudes.

Work at sea

As a supplement to PASCAL, the radiative budget at the sea surface of light in the visible range had been investigated during stations of RV *Polarstern*. By means of different spectrometers, the incoming irradiance and sky radiance had been measured above and in water as well as the backscattered upwelling-directed and water-leaving radiance. Thus, the water colour-containing and remote sensing-relevant information – remote sensing reflectance – had been determined based on these measurements. In addition, the polarization properties of the sky radiance and from the sea upwardly directed radiance had been characterized. The following instruments had been deployed; the corresponding data are summarized in Table 5.1:

- different hyperspectral (UV, VIS, and NIR) radiometers (TriOS Ramses, Ocean Optics, Ibsen FREEDOM VIS) to measure irradiance and radiance,
- a polarimeter (URMS/AMSSP) for water, ice, and atmosphere to measure multi-angle polarized reflectance and radiance,
- a Pandora-2s system to derive atmospheric parameters (AOD, trace gases), and
- a Microtops II sun photometer (AOD)
-

Water samples from the upper mixed layer of the sea (and of melt ponds) have been collected. The spectral (UV, VIS, NIR) absorption of particles and coloured dissolved organic matter (CDOM) have been directly analysed in the wet lab by means of a Psicam and LWCC. GF/F filters with marine particles have been stored for later laboratory analysis of the total biomass (chlorophyll) concentration.

Tab. 5.1: Overview of accomplished measurements (mostly during ship stations). Measured quantities: upwelling radiance below water (L_u^-), downwelling irradiance below and above water (E_d^-, E_d^+), upwelling radiance above water (L_{surf}), sky radiance (L_{sky}), estimated chlorophyll concentration (Chl), CDOM absorption (a_{CDOM}), total absorption (a_{tot}), filtration (GFF). Test, Single, and Auto measurements of URMS are with 10° increment azimuth and elevation.

Nr.	Station	Date (2017)	Start [CET]	End [CET]	Latitude	Longitude	Pangaea Device: RAMSES-1 (Zodiak)	Pangaea Device: FLU (Zodiak)	Pangaea Device: RAMSES-2 (2nd Float)	Pangaea Device: RMASES-3 (Railing)	Pangaea Device: URMS (Railing)	Pangaea Device: Pandora (Railing)	Pangaea Device: WS (Laboratory)
1	PS106_2-2	26.05.	13:10	13:45	61° 6.35`N	3° 17.82`E	L_u^-, E_d^-, E_d^+	Chl	L_u^-, E_d^-	E_d^+, L_{surf}, L_{sky}			
2	PS106_2-2	26.05.	13:10	13:45	61° 6.35`N	3° 17.82`E						11:37–12:52	
3	PS106_3-1	27.05.	11:00	11:30	64° 42.4`N	2° 44.0`E	L_u^-, E_d^-, E_d^+	Chl	L_u^-, E_d^-	E_d^+, L_{surf}, L_{sky}		06:39-09:06	
4	PS106_4	28.05.	08:45	18:46	64° 42.4`N	2° 44.0`E						08:45-18:46	
3	PS106_12-3	29.05.	09:50	11:25	72° 34.56`N	5° 35.41`E	L_u^-, E_d^-, E_d^+	Chl	L_u^-, E_d^-	E_d^+, L_{surf}, L_{sky}			a_{CDOM}, a_{tot}, GFF
4	PS106_12-3	29.05.	06:42	06:45	72° 34`N	05° 35`E					Tests	08:45-18:37	
5	PS106_15-2	30.05.	20:20	20:50	77° 15.71`N	9° 31.57`E				E_d^+, L_{surf}, L_{sky}			a_{CDOM}, a_{tot}, GFF
6	PS106_15-2	30.05.	06:42	18:50	77° 15`N	09° 31`E					Tests		
7	PS106_16-2	31.05.	10:00	10:30	79° 20.3`N	8° 25.9`E	L_u^-, E_d^-, E_d^+	Chl		E_d^+, L_{surf}, L_{sky}	Single		a_{CDOM}, a_{tot}, GFF
8	PS106_17-1	01.06.	12:00	12:40	80° 26.54`N	7° 15.86`E	L_u^-, E_d^-, E_d^+	Chl		E_d^+, L_{surf}, L_{sky}	Single	03:11-16:49	a_{CDOM}, a_{tot}, GFF
9	PS106_18-1	02.06.	14:00	14:30	81° 17.41`N	9° 18.18`E				E_d^+, L_{surf}, L_{sky}			a_{CDOM}, a_{tot}, GFF
10	PS106_24-3	07.06.	09:00	10:20	81° 56.16`N	10° 14.59`E	L_u^-, E_d^-, E_d^+	Chl		E_d^+, L_{surf}, L_{sky}	Single	03:11-16:49	a_{CDOM}, a_{tot}, GFF
9	PS106_25-2	08.06.	09:00	12:15	81° 54.501'N	9° 52.05`E				E_d^+, L_{surf}, L_{sky}		10:38-19:08	a_{CDOM}, a_{tot}, GFF
10	PS106_26-3	09.06.	09:30	10:30	81° 54.51`N	10° 0.679`E	L_u^-, E_d^-, E_d^+	Chl		E_d^+, L_{surf}, L_{sky}		03:10-14:44	a_{CDOM}, a_{tot}, GFF
11	PS106_27-2	10.06.	08:50	10:50	81°54.23`N	10° 0.14`E				E_d^+, L_{surf}, L_{sky}	Auto	06:10-16:25	a_{CDOM}, a_{tot}, GFF
12	PS106_28	11.06.	15:42	15:52	81° 49`N	11° 14`E					Auto	07:05-18:58	
13	PS106_29	12.06.	07:26	12:55	81° 49`N	11° 33`E					Auto	03:10-18:57	

Nr.	Station	Date (2017)	Start [CET]	End [CET]	Latitude	Longitude	Pangaea Device: RAMSES-1 (Zodiak)	Pangaea Device: FLU (Zodiak)	Pangaea Device: RAMSES-2 (2nd Float)	Pangaea Device: RMASES-3 (Railing)	Pangaea Device: URMS (Railing)	Pangaea Device: Pandora (Railing)	Pangaea Device: WS (Laboratory)
14	PS106_30	13.06.	06:38	18:52	81° 49`N	11° 34`E					Auto	03:09-18:53	
15	PS106_31	14.06.	05:27	05:27	81° 47`N	11° 17`E					Tests	12:05-16:41	
16	PS106_32	15.06.	07:49	13:22	81° 43`N	10° 51`E					Auto	12:01-12:29	
17	PS106_33	16.06.	06:38	18:52	80° 41‘ N	10° 28‘ E					Auto	11:32-11:43	
18	PS106_34-1	17.06.	14:00	15:00	80° 59.75‘ N	10° 21.94‘ E	L_u^-, E_d^-, E_d^+	Chl		E_d^+, L_{surf}, L_{sky}	Auto		a_{CDOM}, a_{tot}, GFF
19	PS106_39-1	18.06.	12:30	14:00	80°09.38’N	10°38.54‘ E	L_u^-, E_d^-, E_d^+	Chl		E_d^+, L_{surf}, L_{sky}	Auto		a_{CDOM}, a_{tot}, GFF
20	PS106_41-1	19.06.	07:51	14:07	78°32’N	03°52‘ E	L_u^-, E_d^-, E_d^+	Chl		E_d^+, L_{surf}, L_{sky}	Auto		a_{CDOM}, a_{tot}, GFF

Preliminary results

1. Hyperspectral radiance and irradiance have been measured above and in-water to characterize the available light and its polarized angular distribution. From these measurements, the following light field and apparent optical properties can be deduced:

   a) Vertical profile of the underwater light field and reflectance ratio just below the sea surface,

   b) Hyperspectral water-leaving radiance and remote sensing reflectance,

   c) and, due to different sun positions and wind speeds during the measurements, the actual sea surface reflectance factor as function of wind, waves, sun altitude, and atmospheric conditions.

   d) Furthermore, we collected valuable data for the comparison of different sensors.

2. Inherent optical water properties of water samples have been characterized, i.e., total absorption of all marine particles and absorption of CDOM. In addition, GF/F filters have been stored for later lab analysis of the chlorophyll concentrations. First assessment of the data show expected orders of magnitude for the absorptions in the open sea (measurements during stations on the transect) and comparable low concentrations of CDOM and floating biomass in the polynya, the area of open water surrounded by sea ice (measured during the ice station).

3. During clear sky conditions, several match-ups (of *in-situ* radiometric measurements and water sampling) with Sentinel-3/OLCI and Sentinel-2/MSI imagery could be acquired. A high resolution Sentinel-2/MSI image of the floe is shown in Fig. 5.1. The image illustrates the sea ice cover around RV *Polarstern* during ice station at June 10th 2017 and allows estimating the extent of the floe. The image shows the heterogeneity of the ice and water structure. With respect to ocean colour, such imagery will help analysing adjacency effects of the bright ice over dark water and melt ponds.

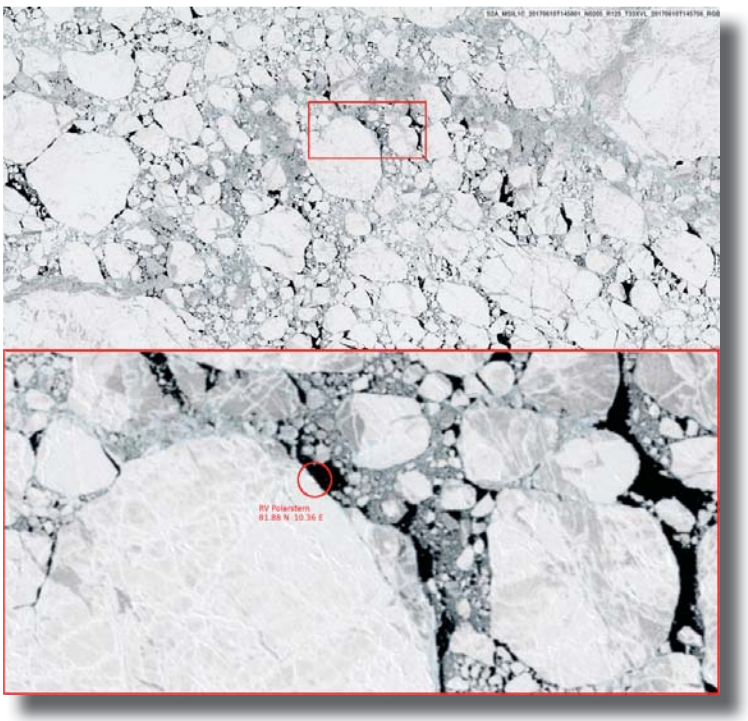

Fig. 5.1: Sentinel-2A MSI image of the ice floe with test site acquired June 10, 2017 at 15:00 UTC with roughly 10 m pixel resolution (contains modified Copernicus Sentinel data [2017] processed by ESA/ HZG). The floe size is approximately 4.1 km in North-South and 3.7 km in East-West directions.

References

Gege P (2004) The water color simulator WASI: an integrating software tool for analysis and simulation of optical in situ spectra. Computers & Geosciences, 30(5), 523-532.

Hieronymi M (2016) Polarized reflectance and transmittance distribution functions of the ocean surface. Optics Express, 24(14), A1045-A1068.

Hieronymi M, Müller D, and Doerffer R (2017) The OLCI Neural Network Swarm (ONNS): A Bio-geo-optical Algorithm for Open Ocean and Coastal Waters. Frontiers in Marine Science, 4, 140.

Hollstein A and Fischer J (2012) Radiative transfer solutions for coupled atmosphere ocean systems using the matrix operator technique. JQSRT, 113(7), 536-548.